Cellulose (2024) 31:10845–10859
https://doi.org/10.1007/s10570-024-06245-5

ORIGINAL RESEARCH

Durability of cellulose nanofibril films examined via residual drying stress measurement

Daniel J. Franke · Ronald C. Sabo · Cody A. Schilling

Received: 14 May 2024 / Accepted: 20 October 2024 / Published online: 27 October 2024

Abstract Cellulose nanomaterials (CNMs) have potential utilization as oxygen barrier layers when applied as the primary component of a single layer in multilayer packaging systems. One limitation of dense CNM films is their lack of durability due to their brittle nature. The durability of cellulose nanofibril (CNF) films was examined through the lens of understanding the residual stress that formed within the films during drying. A beam bending method consisting of drying CNF films on top of a flexible substrate was used to quantify residual stress. It was determined that for two common variations of CNFs (TEMPO-oxidized vs mechanically refined), the residual drying stress was on the order of 50% of the yield strength of the material at a given humidity. Larger residual stress formed within the TEMPO-oxidized CNFs as compared to the mechanically refined CNFs due to the smaller fibril diameters resultant of the TEMPO oxidation production process. The residual stress in the TEMPO-oxidized material was also more sensitive to moisture (humidity) than the mechanically refined material. Various plasticizers were examined for their efficacy in reducing residual drying stress. Triethyl citrate appears more effective in reducing residual stress than common polyols (glycerol/sorbitol), especially when subjecting the films to low humidity. Triethyl citrate in combination with a small amount of polyvinyl alcohol at a total plasticizer content of 30% of the mass of the CNFs resulted in a 75% reduction in the residual stress from the unplasticized state. In this low-stress state, standalone films (10–15 μm) can withstand creasing operations that compromise unmodified (high residual stress) films in terms of their ability to prevent oxygen transmission. Additionally, the low-stress formulation was coated onto a paper substrate resulting in enhanced durability during creasing operations prior to oxygen barrier testing.

Keywords Cellulose nanofibrils · Durability · Residual stress · Oxygen barrier

Supplementary Information The online version contains supplementary material available at https://doi.org/10.1007/s10570-024-06245-5.

D. J. Franke (✉) · R. C. Sabo · C. A. Schilling
Forest Products Laboratory, USDA Forest Service, 1 Gifford Pinchot Dr, Madison, WI 53726, USA
e-mail: daniel.franke@usda.gov

Introduction

Cellulose nanofibrils (CNFs) are emerging as a promising class of sustainable materials for a wide range of applications including packaging, flexible electronics, and high-strength composites (Moon et al. 2011; Tayeb et al. 2018; Hubbe et al. 2017; Wang et al. 2018; Sabo et al. 2016). Cellulose is one of the most abundant natural biopolymers, and through effective utilization can reduce human dependence on environmentally harmful synthetic polymers (Moon et al.

2011; Tayeb et al. 2018; Hubbe et al. 2017). One promising application of CNFs is as the oxygen barrier layer within packaging materials. When dried into a film or deposited onto a substrate (paper or another polymer), they form a dense layered structure that has high resistance to gas transport. This resistance is attributed to the large aspect ratio of the nanoparticles and the extensive inter- and intramolecular hydrogen bonding that is formed within the layers (Moon et al. 2011; Tayeb et al. 2018; Hubbe et al. 2017). While researchers have shown that adding cellulosic nanomaterials (CNMs) to polymers can increase their oxygen resistance, recent studies have concluded that the material was most effective as a barrier when the fibrils are assembled in a densely packed layer as the primary component (Wang et al. 2018). This was attributed to the observation that low levels of loading achievable in standard polymers have not been shown to increase oxygen resistance to the levels needed to reach the performance of standard barrier materials (Wang et al. 2018).

Films composed of a dense layer of cellulose nanomaterials have shown potential as an effective oxygen barrier. However, the physical nature of said dense layer has distinct limitations. One primary limitation is the lack of durability (Hubbe et al. 2017). A dense layer of entangled stiff nanoparticles with extensive hydrogen bonding results in brittle films (Hubbe et al. 2017; Wang et al. 2018; Mokhena et al. 2021). Mechanical testing of neat CNF films often results in tensile failure at strains less than five percent (Mokhena et al. 2021). The formation of cellulose nanomaterial films involves the removal of large amounts of water during drying leading to significant residual stress formation within films, which contributes to the lack of durability (Mariani et al. 2019; Qing et al. 2012; Klockars et al. 2023; Greca et al. 2023). The CNM layer will be subjected to creasing/folding operations when used in paper-based packaging. The layer must remain intact after creasing to function as a barrier. Creased barrier testing of CNM films is largely absent from academic literature. Limited studies examining the effect of creasing on barrier properties of mechanically refined cellulose films have been reported (Fein et al. 2021; Hasan et al. 2021; Tayeb et al. 2020a). It is hypothesized that the lack of reported investigation of creased films was due to the destruction of CNM barrier layers when creasing, *i.e.*, a lack of reporting of negative results.

Plasticization of cellulose nanomaterial films

Several biobased materials have been proposed as plasticizers in CNM films. Biobased and biodegradable additives are the ideal route for enhancing CNMs while maintaining the inherent sustainability benefit. One common approach is the addition of polyols such as glycerol, xylitol, and sorbitol (Azeredo et al. 2010; Hansen et al. 2012; Soni et al. 2016; Csiszar and Nagy 2017; Herrera et al. 2017; Fernández-Santos et al. 2021; Aulin et al. 2022). Researchers have shown the addition of sorbitol or glycerol can increase the strain to failure of films, with larger loadings of the polyol leading to larger strain. This has been attributed to the polyol disturbing the hydrogen bonding between fibrils and allowing them to slide past each other during deformation. However, as more polyol is added the film will start to lose its ability to prevent oxygen permeation (Hansen et al. 2012). It is hypothesized that the plasticizer can start to create channels that oxygen can permeate through. Aulin et al. (2022) showed that oxygen permeation started to increase above 20% loading of sorbitol and glycerol, with glycerol causing a larger increase in oxygen permeation than sorbitol. The utilization of glycerol or sorbitol has allowed for strain to failure values of around 10–12% to be achieved while still maintaining oxygen barrier properties.

Another approach is the addition of other water-soluble polymers to the CNM film. When the polymer occupies the space between fibrils it can lead to more ductile deformation since the polymers tend to be more ductile than entangled cellulose nanofibrils. The common polymers that have been examined in this application are polyvinyl alcohol (PVOH) (Hakalahtia et al. 2015; Forti et al. 2021; Nuruddin et al. 2021), carboxymethyl cellulose (CMC) (Fernández-Santos et al. 2022), and polyethylene oxide (PEO) (Ma et al. 2021). Other studies have been performed with nano latex particles (Kumar et al. 2016), poly[poly(ethylene glycol methyl ether methacrylate)-co–N,N-dimethylacrylamide] (Benítez et al. 2016), and colloidal lignin nanoparticles (Farooq et al. 2019). All studies suggest that adding more polymer increases the ductility of the film. Several studies have reported strain to failures around 20% with up to 50% addition of polymer. However, these studies do not examine the effect of polymer addition on oxygen barrier properties. Adding a substantial amount of

polymer may drive the oxygen permeability properties of the film toward the properties of the polymer itself.

Another potential class of plasticizers for CNM films are citrate esters, which are derived from the natural compound citric acid. This group of plasticizers does not present any toxicity, is approved for personal care and food contact, and is known for fast biodegradation (Rahman and Brazel 2004). These attributes make them a suitable candidate for compostable/biodegradable food packaging. Triethyl citrate (TEC) has been used as an effective plasticizer in cellulose derivatives such as cellophane and cellulose acetate (Teixeira et al. 2021, Erdman et al. 2021). Interestingly, the examination of citrate esters in nanocellulose films is limited. Only one publication by Reshmy et al. (2021) has examined the utilization of triethyl citrate in a nanocellulose film. The nanocellulose examined was derived from jackfruit peel using an acid hydrolysis process. No examinations of triethyl citrate in wood-based cellulose nanofibrils have been performed in the available literature. Several studies have also used citrate esters to plasticize the polymer matrix that low loading weights of cellulose nanomaterials have been composited with (Jung et al. 2020; Cindradewi et al. 2021; Tian et al. 2022; Arrieta et al. 2015). One goal of the current study was to examine the plasticizing effect of triethyl citrate in cellulose fibril-to-fibril interactions.

Residual stress in cellulose nanomaterials

Researchers have proposed and observed that large residual stresses form during the drying of nanocellulose materials (Mariani et al. 2019; Qing et al. 2012; Klockars et al. 2023; Greca et al. 2023). The conventional understanding of drying of cellulosic fibers in papermaking suggests that capillary bridges and capillary pressures are responsible for pulling fibers together (Greca et al. 2023). In the case of nanoscale fibers, the capillaries are substantially smaller, and thus the capillary pressures during drying are much higher. Coupled with the relatively large amount of molecular contact between the nanoscale particles, the large capillary pressures lead to large amounts of internal stress upon drying of cellulose nanomaterials (Klockars et al. 2023; Greca et al. 2023). Large distortions in solution-cast nanocellulose films are often observed in literature, and residual stress has been acknowledged but not widely studied. Only recently have two studies examined the stress that formed in cellulose nanocrystal (CNC) films (Klockars et al. 2023; Greca et al. 2023). A better understanding of the residual stress formation in cellulose nanofibrils is needed given the potential impact on the durability of the material. The objective of the current work was to quantify the effects of plasticizers and humidity on the residual stress that forms in two common types of cellulose nanofibrils, TEMPO-oxidized CNFs and mechanically refined CNFs.

Background on quantification of residual stress in coatings

The first quantitative measurement of residual stresses in coatings has been attributed to research by Stoney (1909). This work was the first to present the concept that residual stress formation in coatings can deform flexible substrates and therefore the known stiffness of the substrate can be used to quantify the stress in the coating. The history of how this concept evolved into the study of residual stress of solvent-based coatings using flexible substrates was well described by Payne et al. (1998). The most common approach has been to apply a solvent-based coating to a cantilevered beam and use a standard plate and beam theory to quantify the internal stress. The equation most commonly used was derived by Corcoran (1969) and takes the following form:

$$\sigma = \frac{dEt^3}{3cL^2(t+c)(1-\vartheta)} + \frac{dE_c(t+c)}{L^2(1-\vartheta_c)} \quad (1)$$

where σ is the residual stress in the coating, d is the deflection of the cantilevered beam at the end of the beam, E is the modulus of elasticity of the substrate, t is the thickness of the substrate, c is the thickness of the coating, L is the length of the beam, ϑ is the poisons ratio of the substrate, E_c is the modulus of elasticity of the coating, and ϑ_c is the Poisson's ratio of the coating. The assumptions involved with the use of this equation are spherical defection of the beam, deformation within the elastic limits of the coating and substrate, isotropic mechanical properties, and good adhesion between coating and substrate. Additionally, the width of the beam must be much larger than the thickness of the coating in order for shear and peeling stress near the edge of the coating to

become insignificant. The determined stress value is a biaxial in-plane tensile stress averaged through the coating's thickness (Corcoran 1969).

Methods

Materials

The two cellulose nanofibril materials examined are TEMPO ((2,2,6,6-Tetramethylpiperidin-1-yl)oxyl)-oxidized CNFs (TOCNs) produced at the Forest Products Laboratory in Madison WI, and mechanically fibrillated CNFs (sometimes referred to as cellulose microfibrils-CMFs) produced at the Process Development Center at the University of Maine in Orono, ME. The Process Development Center classifies the material as their 90% fines version (Kelly et al. 2021). Both materials have been studied in the scientific literature (Moon et al. 2011; Tayeb et al. 2018; Hubbe et al. 2017; Wang et al. 2018; Reiner and Rudie 2017; Kelly et al. 2021) and are representative of two common variations (TEMPO oxidation pretreatment vs. mechanical disk-type refining alone) of wood-based cellulose nanofibrils. Using a TEMPO oxidation pretreatment before fibrillation results in a material characteristic of small uniform fibrils with diameters on the order of 10 nm that have an abundance of sodium carboxylate groups on the surface of the fibrils (Reiner and Rudie 2017). The mechanically fibrillated material (without oxidation) is characteristic of a hierarchical branched structure with elementary fibrils at the nanoscale extending from large fibrils at the microscale (Kelly et al. 2021). One difference between the two CNF materials is that the oxidation process leaves carboxylate groups on the surface of the TEMPO CNFs. The TEMPO CNFs used in this study had a carboxyl level of 1.47 mmol/g (dry basis) as determined by a modified TAPPI T237 method (Reiner and Rudie 2017). The mechanically refined material is not known for having a significant amount of carboxylate groups as evident by the low surface charge of the material measured by Kelly et al. 2021. The plasticizers examined included sodium carboxymethyl cellulose (90,000 average M_w purchased from Sigma Aldrich), a biobased polyvinyl alcohol derived from sugarcane (24,000 average M_w provided by Bioplastics International), D-sorbitol (purchased from Sigma Aldrich), glycerol (J.T. Baker Brand), and triethyl citrate (Citroflex™ 2 manufactured by Aurorium). Select CNF formulations were coated on the gloss side of a commercial machine glazed 50 g/m^2 basis weight food wrapping paper. A starch base layer (PENFORD® GUM 280, manufactured by Ingredion) was applied to the paper prior to CNF coating.

Measurement of residual drying stress

The method used to quantify the residual stress in CNF films was similar to the method utilized by Greca et al. (2023) and Klockers et al. (2023) to measure drying stress in cellulose nanocrystals. The beam deflection method (Fig. 1) involved constraining 10 mm of a 50 mm long Corning® 0211 No. 1 thickness borosilicate glass coverslip (50 mm long, 10.5 mm wide, 0.145 mm thick) to create a 40 mm long flexible substrate. The coverslip was fixed to a rigid glass slide (deflection reference point). CNF suspensions were applied to the top of the coverslip and allowed to dry at room temperature (23–25°C) and humidity (30–40% RH). A select set of neat TOCN samples were also dried in a laboratory oven (Thermo Scientific Model 666) at 95°C for a drying rate comparison. The mechanically fibrillated CNFs/CMFs were applied as a 2 wt.% suspension to the coverslip at a total suspension mass of 0.5 g for each sample. For most of the samples, the TOCNs were applied as a 1 wt.% suspension to a

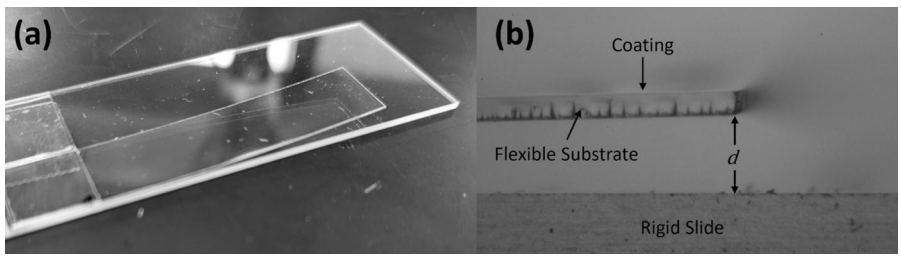

Fig. 1 Beam bending method used to quantify residual stress in coatings: **a** cantilevered coverslip on slide, **b** optical microscope image of the deflected end of the flexible coverslip

total mass of 0.8 g to each coverslip. Select additional samples were made using TOCN suspension masses of 0.4 g and 1.2 g to alter the thickness of the coating. The two CNF types are applied at different suspension concentrations because they have different rheological properties. The specific concentrations were chosen to provide adequate mixing of the plasticizers while still attempting to maintain high solids contents. After drying, samples were conditioned at specific relative humidities in humidity rooms for a minimum of eight hours and measured at the specific humidity using a microscope to image the deflection of the coverslip with reference to the rigid slide (Fig. 1b). To measure the deflection, the number of pixels between the bottom of the coverslip and the top of the slide was measured in ImageJ and converted to a length value using the known scale of the image. After imaging, the thickness of each coverslip and coating was measured using a digital micrometer. Additionally, the modulus of elasticity (E term in Eq. 1) of the borosilicate glass coverslips was examined using a Dynamic Mechanical Analysis system (TA instruments DMA Q800). Further detail on the stiffness verification of the flexible substrate is contained in the supplemental material.

The effect of the additives on the residual stress formation was examined at loading percentages of 10, 20, and 30% of the dry mass of the TEMPO-oxidized CNFs all at a fixed humidity of 50% RH. An additional combination of 20% of the triethyl citrate (TEC) and 10% of the PVOH (30% total loading of the dry mass of the cellulose) was also examined at 50% RH. All plasticizers were mixed into the liquid suspension using a magnetic stirrer. The polymer plasticizers (CMC and PVOH) were first made into 5wt.% solutions and then mixed into the CNF suspension. In the mechanical grade of CNFs, 30% loadings of PVOH, TEC, glycerol, and the combination of 20% TEC and 10% PVOH were all examined at 50% RH. A humidity sweep study of the neat formulations (both TOCNs and Mech. CNFs), as well as 30% loadings of TEC and glycerol, was performed at humidities ranging from 20% RH to 80% RH based on the controlled humidity rooms available. The exact humidity of each humidity room was measured using a humidity monitor (Sensirion SHT31) at the time of sample imaging. Five sample replicates were prepared for every experimental condition.

Film preparation and paper coating

Standalone TOCN films were cast in polystyrene Petri dishes in order to examine their oxygen barrier properties and durability. Suspensions were diluted to less than 0.5 wt.% solids in terms of cellulose, and plasticizers were added at specified loadings. Formulations tested for durability consisted of neat TOCNs, TOCNs with 20% TEC combined with 10% PVOH, and TOCNs with 10% PVOH alone. Formulations of neat TOCNs and TOCNs with 20%TEC + 10% PVOH were also coated onto a 50 g/m^2 commercial food wrapping paper using 1 wt.% solids suspensions. Coating was performed using an automatic film coater (model MSK-AFA-III, MTI Corporation, Richmond, CA, USA) and dried with the attached forced air top heater. Papers were cut to approximately 18 cm wide and 33 cm long with the length and coating direction parallel to the machine direction of the paper. The papers were held onto the coater by vacuum and by taping the perimeter to the vacuum plate. A 100 mm wide doctor blade was used to apply the coatings by spooning excess coating solution in front of the doctor blade. The gap on the doctor blade was set to 1.2 mm for applying CNFs and CNF-polymer mixtures and was set to 10 µm for starch layers. Coating speeds were maintained at 10 mm/s for CNFs and CNF-polymer mixtures and at 30 mm/s for starch. The forced air for drying was heated to a set point of 35 °C, and the papers were left taped and vacuumed to the plate until dry with the drying lid closed.

Creased oxygen barrier testing

All samples were conditioned at 50% relative humidity (RH) prior to creasing. Standalone films were creased in accordance with the TAPPI T512 standard. This involved two perpendicular creases folded in opposite directions with respect to the bending axis of the film and creased with the standard 2.04 kg weighted roller. Coated paper samples were creased using the TAPPI standard roller but were tested with single folds considering the bending direction with respect to the neutral axis of the paper, *i.e.*, folding the sample towards the coated side of the paper versus folding away from the coated side.

Oxygen permeability testing of free-standing films and coated papers was conducted via oxygen transmission measurements performed on a Mocon

OX-TRAN 2/22L (Ametek MOCON, Brooklyn Park, MN, USA) in accordance with ASTM D3985. The thickness of free-standing films was measured in ten locations within the test area prior to testing using a digital micrometer. A test cell with a 50 cm^2 testing area was used for free-standing films, and for coated paper samples, a cell with a 5.64 cm^2 testing area was used. Free-standing films were tested at 23°C and 30%, 50%, and 70% relative humidity. Coated paper samples were tested at 23°C and 40% and 60% relative humidity. Sample runs were programmed for 60-min test cycles with a convergence criterion of 2% across the last three test cycles at each humidity step to ensure sample equilibrium. An instrument re-zero was performed at the beginning of each sample run for 60 min and was repeated every eight testing cycles throughout the full sample convergence run. Two replicates were performed for each sample type. The permeability of freestanding films was calculated by multiplying by the thickness of the film and dividing by the measured pressure of the system. For coated paper samples, the values are presented as transmission rates at a given coating weight of the CNF barrier layer. The coating weight was determined by cutting coated papers to a known area (10.16 cm by 25.40 cm) and measuring the mass compared to the mass of the paper with the starch base layer.

Tensile testing of films

CNF films cast in Petri dishes were cut into tensile specimens using an ASTM D-638-V tensile specimen die. For tensile testing, mechanically fibrillated samples were cast to film thicknesses of 100–150 µm, and the TOCN samples were cast to thicknesses of 32 µm. The thickness of TOCN samples that can be cast was limited by large drying deformations in thicker samples. Tensile specimens were made from both the mechanically refined CNFs and TEMPO-oxidized CNFs in their neat conditions and plasticized with 20%TEC and 10% PVOH. Eight tensile bars were cut from each specimen type. Tensile testing was performed on a load frame (Instron 5566 Universal Testing Machine, Instron, Norwood, MA, USA) in a humidity-controlled room (50% RH) after samples had been conditioned to 50% relative humidity. A video extensometer system (Epsilon ONE-130PT-210, Epsilon Technology Corp, Jackson, WY, USA) with a gauge length of 0.762 cm was used to measure elongation. All tensile tests were performed at a rate of 2.54 mm/min (0.1 in/min).

Scanning electron microscopy imaging of coating surfaces

The surfaces of CNF coated papers were analyzed by scanning electron microscopy (SEM) to interrogate the impact on coating integrity resulting from the creasing procedures. Samples of approximately 1 cm^2 were cut from coated papers. Samples consisted of both a neat and plasticized (20%TEC + 10%PVOH) TOCN coating creased towards the coating side of the paper, as well as a plasticized TOCN coating creased away from the coating side. The samples were carefully mounted on aluminum stubs using double-sided carbon tape, followed by sputter coating with gold to enhance conductivity. SEM images were captured on a Ziess Evo LS 15 SEM (Carl Zeiss, LLC, UK) operating at an accelerating voltage of 3 kV. Multiple images were taken along the length of the creases to ensure images were representative of the sample.

Results and discussion

Implementation of Eq. 1

All terms in Eq. 1 are needed to determine a residual stress value. The most critical terms, such as length of the beam (L), deflection (d), thickness of the flexible substrate (t), and thickness of the coating (c) are physical measurements that were measured directly for each sample. The coating thicknesses for the TOCN samples were on the order of 12–15 µm and the mechanically fibrillated samples were on the order of 25–30 µm. The flexible glass substrates were all within the range of 142–145 µm thick. The modulus of elasticity (E) of the glass substrates was measured using compliance tests on a commercial DMA system that produced an average value of 69 GPa. This value was within the range of reported values for borosilicate glass (Bootjomchai et al. 2014, MatWeb.com 2024). The Poisson's ratio of the flexible substrate (ϑ) was taken to be 0.2 (MatWeb.com 2024). The modulus of elasticity (E_c) of TOCN films and the mechanically refined CNF films were taken from tensile testing results of films made of the two materials. These

were determined to be 5.5 GPa and 3.4 GPa for the TOCNs and the mechanically refined grades respectively. The Poisson's ratio of all CNF coatings (ϑ_c) was taken to be 0.3 (Nakamura et al. 2004). The stiffness and Poisson's ratio of the CNF coating may vary slightly depending on plasticizer content. The second term in Eq. 1 had minimal effect on the residual stress value since the stiffness of the coating was less than a factor of ten smaller than the stiffness of the glass. Therefore, any changes in stiffness and Poisson's ratio were assumed insignificant. The second term of Eq. 1 was dropped entirely in several prior studies (Greca et al. 2023; Klockars et al. 2023).

Residual drying stress

The first examination involved the effect of drying rate on residual stress formation through the direct comparison of neat TOCN samples dried at room temperature versus in a laboratory oven at 95°C. In the oven, the films took on the order of 15 min to dry, while at room temperature, the films took on the order of 6–8 h to dry. The deflection of the coverslips, and thus the internal stress, was nominally the same for both conditions with 68.9 ± 5.9 MPa stress forming in the oven-dried samples and 69.4 ± 5.5 MPa at room temperature when measured at 30%RH (condition of room the samples were dried in). The uncertainty reported and shown in all images is either the standard deviation in the stress values of the five samples prepared at each condition or the Gaussian propagation of uncertainty using estimated uncertainties for all the values in Eq. 1. The larger of the two uncertainty values was reported. In most cases, the deviation within the five samples at one condition was greater than the Gaussian propagation of Eq. 1. Further information on the propagation of uncertainty estimation is contained in the supplemental material file. The second examination involved the effect of coating thickness on residual stress. Three targeted TOCN coating thicknesses ranging from 8 µm to 20 µm showed that there was no statistical difference in the residual stress due to thickness variations in this range. Producing thickness outside of this range while keeping the solids content of the suspension consistent is difficult due to the low solid content and volumes of suspension required.

The residual stress that formed in the neat formulations of both CNF materials when the samples were conditioned at a range of humidities is shown in Fig. 2. Larger residual stress formed in the TOCN samples than in mechanically refined samples. The TOCN material is characteristic of uniform nanosized fibrils, while the mechanically refined material has larger microscale fibrils with nanoscale branches. This suggests that there are more nanoscale capillaries with larger capillary pressure and more nanofibril-to-nanofibril contact in the TOCN material that led to the larger residual stress. Additionally, the carboxylate groups on the surface of the TOCN fibrils may alter how the drying process occurs and how the residual stress forms. The carboxylate groups may form stronger hydrogen bonds with adjacent hydroxyl groups which could lead to higher residual stress formation. The molecular scale roughness of the larger less refined fibers within the mechanically refined material should be larger than the molecular scale roughness of the TOCN fibers. Molecular scale roughness has been proposed as a significant factor for residual stress formation as a lower roughness leads to more intimate contact between fibers leading to larger residual stresses (Greca et al. 2023). In both materials, the residual drying stress at low relative humidities was on the same order of magnitude as the yield stress and ultimate tensile strength (UTS) of standalone films (Table 1). This suggests that the residual stress may contribute to the failure of these materials during deformation.

Humidity appears to have a larger effect on residual stress in the TOCN material than in the mechanically refined material (Fig. 2). This may be due to the

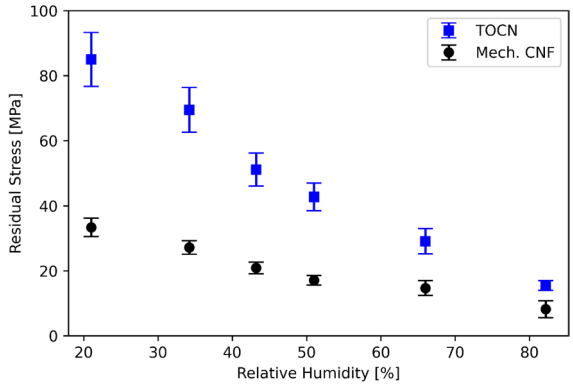

Fig. 2 The effect of relative humidity on the internal residual stress of CNF films. Note: "TOCNs" is the TEMPO-oxidized CNFs and "Mech. CNFs" is the mechanically refined grade

Table 1 Mechanical Properties of CNF films determined via tensile testing at 50% relative humidity

	Yield stress [MPa]	Ultimate tensile stress [MPa]	Strain at failure [%]	Modulus of elasticity [GPa]
TOCNs	120	190	8	5.5
Mech. CNFs	60	155	20	3.4

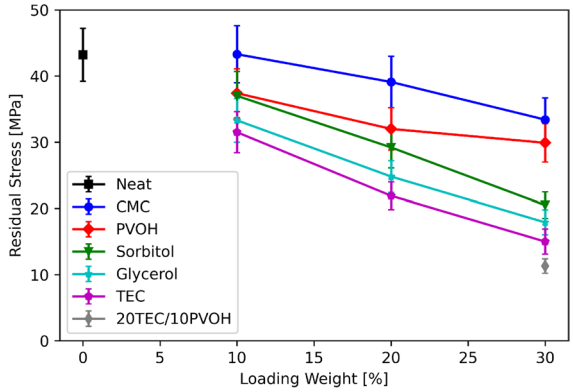

Fig. 3 The effect of plasticizer loading on the residual drying stress of TOCN thin films at 50% relative humidity

greater hydrophilicity of the TOCN material due to its surface chemistry (carboxylate groups) as well as the uniform nanoscale fibril size allowing better access of water to functional groups. As the film absorbs water at higher humidity, the water plasticizes the film and allows the material to relax. The deflection measurement was also an interesting way to visualize how plasticization by water affects the ability of CNF films to prevent the diffusion of oxygen molecules. A significant limitation of using cellulose nanomaterials as an oxygen barrier is that their barrier properties deteriorate at high humidities (Hubbe et al. 2017; Wang et al. 2018; Tayeb et al. 2020b). Take for example the TOCN samples near 20% relative humidity, in this condition, the film constricted enough to deflect the end of the glass beam 2.3 mm from its original position. Above 80% RH, the film has relaxed to the point where the beam was only deflected 0.6 mm (Fig. 1 of the supplemental material file). This illustrates how the fibrils are constricted into a tight-knit mesh in the dry condition and relax into a loose-knit mesh upon water absorption. Relaxation of the mesh of fibrils suggests it would be easier for oxygen molecules to migrate through the mesh of fibrils. The packing density and lack of free volume are what appear to affect the oxygen transmission through a CNF layer (Wang et al. 2018; Chowdhury et al 2019). This was consistent with the oxygen transmission data measured for TOCN films of the same thickness as the ones on the deflected beams that allowed on the order of 0.1 cc/m^2day of oxygen transmission at 20% RH, but on the order of 100 cc/m^2day at 80% RH.

One goal of this work was to examine how an array of different plasticizers alters the residual stress formation during drying of a CNF film. This assessment, performed at a consistent relative humidity (50%) with increasing amounts of plasticizer loading, is shown in Fig. 3. The polymers (CMC/PVOH) were not as effective at reducing the residual stress as the polyol plasticizers (sorbitol/glycerol) or triethyl citrate. This suggests the smaller molecules were better at disrupting the fibril-to-fibril interaction and allowing the fibrils to slide past each other during film formation. The water-soluble polymers did provide some stress relaxation by disrupting fibril-to-fibril interaction during drying, and when dried alone (without CNFs), formed films with lower residual stress (less than 5 MPa). PVOH produced a greater reduction in the residual stress than CMC, which is consistent with PVOH having greater ductility/flexibility than sodium CMC (a brittle polymer in solid form) (Yadav et al. 2013).

In terms of residual stress reduction, glycerol was a slightly better plasticizer than sorbitol at a given loading mass, which has been observed before in mechanical testing of CNF films (Aulin et al. 2022). Prior researchers proposed that with standard polyol plasticizers (glycerol, sorbitol, mannitol, xylitol), the plasticizing efficiency increases with decreasing molecular mass as there are more plasticizing molecules for a given loading mass (Mathew and Dufresne 2002). Triethyl citrate (TEC) appeared slightly better at reducing residual drying stress than glycerol in CNF films. No existing scientific literature has compared the effects of glycerol and TEC in CNFs. However, Teixeira et al. (2021) have shown that TEC was more effective than glycerol in plasticizing cellulose acetate. The explanation provided by Teixeira et al. was that TEC is a larger molecule than glycerol, and therefore TEC created larger spacing between the cellulose acetate polymer chains. The more likely explanation

in the case of drying stress formation is that TEC is often used as an emulsifier and can act as a surfactant in water (Monfort et al. 2012). Figure 2 in the supplemental material file shows a droplet of water saturated with TEC on a glass surface compared to neat water and water with glycerol. The TEC appears to reduce the surface tension of the water, changing the contact angle from around 90° in the neat and glycerol droplets to around 45° in the TEC droplet. Reducing surface tension was shown to reduce capillary forces and residual stress in other solvent drying systems (Wedin et al. 2005). Therefore, TEC may reduce residual stress through both methods, allowing fibrils to slide past each other and reducing capillary pressure. Further investigation of surfactant-based residual stress reduction is warranted.

The slightly hydrophobic nature of TEC caused challenges when plasticizing TOCN at high loading amounts. The TEC tended to segregate from the TOCN film and form visible droplets on the surface at 20–30% loading (shown in Fig. 3 of the supplemental material file). The segregation may be due to the relatively low solubility of TEC in water (6.5g/cm^3), so as the water evaporates, the TEC will start to segregate from the system. This prompted the addition of a polymer to the suspension to provide both better compatibilization of the system and occupy space between fibrils to block migration/segregation. This was examined by adding a 10% loading of PVOH along with a 20% loading of TEC to provide a combined 30% loading. This situation appeared to provide the most significant reduction in residual stress formation with an approximate 75% reduction in residual stress from the neat condition (Fig. 3). The PVOH appears to have a compatibilization effect on the TEC in the suspension. Prior research has shown that TEC can provide a small plasticizing effect in PVOH, *i.e.*, the materials have some degree of compatibility (Ahmad Zuber et al. 2019). No segregation of TEC was observed in the samples produced with the addition of PVOH. It was hypothesized that by containing the TEC within the system it can either provide more of a plasticizing effect in fibril-to-fibril interaction and/or plasticize the PVOH polymer chains between fibrils leading to an enhanced reduction in residual stress.

No segregation/migration of TEC was observed in the mechanically fibrillated CNF films at 30% loading. This may be due to the hierarchical branched nature of the mechanically fibrillated material impeding the migration of TEC molecules to the film surface during drying. Furthermore, the mechanically fibrillated CNFs do not have the surface carboxylate groups that the TOCNs do, which may affect TEC compatibility. The residual stress results using various plasticizers at 30% loading in mechanically fibrillated CNF films when tested at 50% RH are shown in Fig. 4. The method is not able to capture a difference in the effect of plasticizers (TEC/Glycerol) on the residual stress at 50% RH. The addition of PVOH does not appear to aid in TEC plasticization, which is consistent with the observation that no TEC appears to segregate at 30% loading. The plasticizers do have a measurable positive effect compared to the polymer (PVOH) alone. The plasticizers produce a similar 75% reduction in residual stress from the neat condition for the mechanically fibrillated CNF films at 50% relative humidity.

The 30% loading conditions of TEC and Glycerol were examined at a range of humidities to further determine their effect on residual stresses in CNF films (Figs. 5 and 6). It was observed that the TEC has a larger effect on the internal stress at lower relative humidities, but as the humidity increases above 50% RH the TEC and Glycerol have a similar effect on the internal residual stress. Glycerol is hydrophilic which allows it to more effectively utilize the available water to plasticize the material. This is consistent with prior studies on plasticization of starch that concluded that smaller molecular weight polyols lead to increased water absorption, *i.e.*, greater water absorption with glycerol compared to sorbitol or mannitol (Mathew and Dufresne 2002). In the absence of

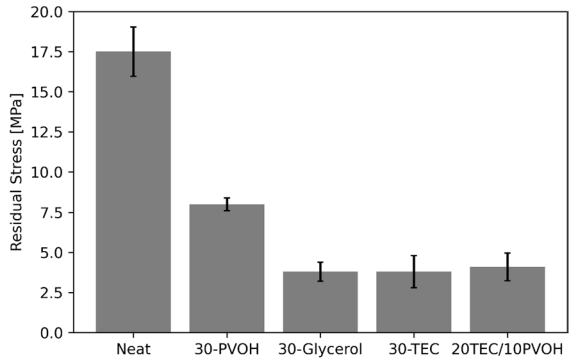

Fig. 4 Effect of 30% loading of plasticizers in the mechanically refined CNFs at 50% relative humidity

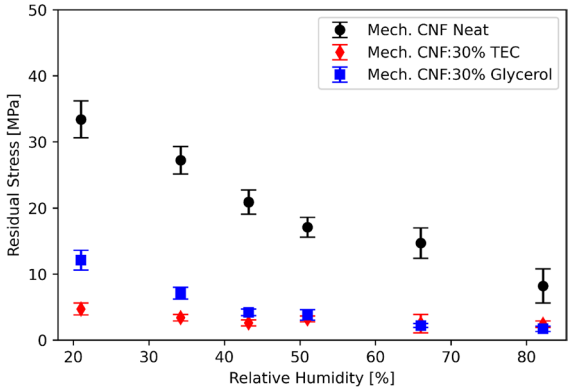

Fig. 5 The effect of the combination of humidity and plasticizer type on the residual stress in mechanically refined CNFs

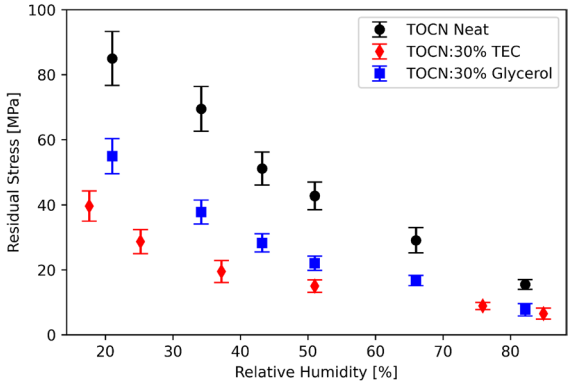

Fig. 6 The effect of the combination of humidity and plasticizer type on the residual stress in TEMPO-oxidized CNFs

water, the TEC appears more effective at plasticizing. This is important because to form the most effective oxygen barrier, the CNF film must have enough water removed from it that the fibrils form a high packing density mesh of fibrils with low free volume (Wang et al. 2018; Tayeb et al. 2020a, b (2), Chowdhury et al. 2019). This occurs when subjecting CNF films to low humidities, *i.e.*, the condition at 20% RH is closer to the desired condition of the material (absence of water in the CNF film) if utilized as an oxygen barrier. A potential approach to producing a CNF oxygen barrier layer that is humidity resistant (effective across a range of humidities experienced during application) is to chemically crosslink the film in a dry state. TEC appears more effective at reducing the residual stress in said dry state. It appears that the ideal scenario is crosslinking the fibrils in a low residual stress state so that the residual stress is not locked into the structure of the film. However, this area of research needs further investigation. Teixeira et al. (2021) also determined that glycerol leads to higher water vapor transmission rates in cellulose acetate films when compared to triethyl citrate. Therefore, the hydrophobic nature of TEC has a potential impact on the prevention of water degradation of barrier properties of CNFs.

Oxygen permeability and durability

Enhanced durability of oxygen barrier layers made of dense cellulose nanomaterials is one practical objective of understanding residual stress formation in CNM films. It was hypothesized that a reduction in the embodied stress in a film can reduce the tendency for CNF films to crack under additional applied stress. The concept was examined by studying the oxygen barrier properties of creased and uncreased TOCN films using high and low residual stress formulations. TOCN films were utilized for this investigation because they are more brittle than the mechanically refined grade of CNFs/CMFs (Table 1). The mechanically refined grade had some level of durability due to its hierarchical nature, *i.e.*, there are still larger less refined fibers at the microscale that provide better durability. This makes the TOCNs more interesting to examine from a durability standpoint since it is the less durable material and tends to have better oxygen barrier properties (Table 2) than the mechanically refined grade due to lower free volume resultant of the uniform nanoscale diameters of the

Table 2 Oxygen permeability results for casted freestanding CNF films

All permeation values are in units of $cm^3 \mu m/m^2 day \cdot atm$

Relative Humidity	TOCNs Neat	TOCNs + 30% Glycerol	TOCNs + 20% TEC + 10% PVOH	Mechanically Refined CNFs
30%	6.2 ± 2.5	62 ± 7.9	7.6 ± 1.7	520 ± 66
50%	26 ± 5.0	820 ± 28	28 ± 14	550 ± 62
70%	410 ± 93	8500 ± 5200	240 ± 57	1200 ± 290

fibrils. The oxygen barrier properties of cast TOCNs (Table 2) suggest that it can be classified as a "very high" (Wang et al. 2018) oxygen barrier at humidities below 50%. Above 50% relative humidity, oxygen barrier performance degrades significantly, which is consistent with existing literature. The addition of 30 wt.% of glycerol appeared to reduce the effectiveness of the TOCNs as an oxygen barrier and exacerbated the effect of humidity on the degradation of the barrier properties. On the other hand, TEC did not appear to have a significant effect on the oxygen barrier properties of the TOCNs when in its compatibilized low residual stress combination with PVOH. This suggests that internal stress in CNF films is not tied directly to oxygen barrier properties.

The average oxygen permeability (cm^3·µm/m^2·day·atm) of casted TOCN films (10–15 µm thick) after creasing with a weighted roller in accordance with the TAPPI T512 standard is reported in Table 3. The neat TOCN films (high residual stress) produced oxygen measurements above the limit of the permeation equipment after creasing. An above-range test means that more than 2500 cc/ m^2·day reached the sensor during testing, which is the result of crack formation in a CNF film allowing oxygen through. An example image of the surface of a sample that was creased and damaged (above-range oxygen) is shown in Fig. 7. The lowest residual stress formulation (20%TEC + 10%PVOH) was able to be creased without a significant change in the oxygen permeability when compared to the uncreased films. This suggests that no cracking occurred during creasing that would allow for oxygen to pass through. To the best of the authors' knowledge, no readily available studies have subjected a TEMPO-oxidized CNF film to a creasing operation without a reduction in oxygen barrier performance. Additionally, TOCNs with a 10% addition of PVOH also failed the oxygen transmission testing when creased (cracking). This suggests that the small addition of polymer was not responsible for making

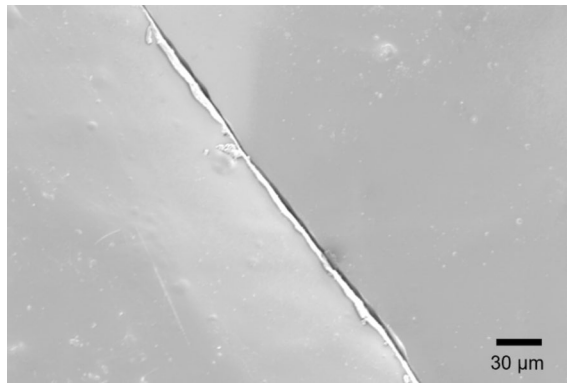

Fig. 7 Scanning electron microscope image of the surface of a fractured CNF film

the 20%TEC + 10%PVOH sample durable enough to be creased, and therefore, the plasticizer (TEC) was critical for reducing residual stress and enhancing durability. As shown in Fig. 3, the neat and 10% PVOH formulations have residual stresses near 40 MPa (50% RH) while the 20%TEC + 10%PVOH formulation has a residual stress around 11 MPa (50% RH). It should be noted that the residual stress in cast films will not be the same as the residual stress in films attached to a glass coverslip due to the different constraining effects of the substrate. The aforementioned values are meant to describe a trend in the reduction of residual stress formation through the addition of plasticizer, not the exact values of residual stress in the cast films.

One potential application of CNFs is as an oxygen barrier layer coating on paper-based packaging. TOCN formulations were blade-coated onto a paper substrate with a starch base layer to test their durability. The starch base layer was utilized as a low-cost material to fill the porosity of the paper to create an even coating surface and thus a more continuous film of the oxygen barrier material (CNFs). The CNF coatings were determined to have an average coating

Table 3 Oxygen permeability results for free standing TOCN films creased via the TAPPI T-512 method

All permeation values are in units of cm^3µm/m^2day·atm

Relative Humidity	TOCNs Neat Uncreased	TOCNs Neat Creased	TOCNs + 20% TEC + 10% PVOH Creased	TOCNs + 10% PVOH Creased
30%	6.2 ± 2.5	Above Range	6.1 ± 0.5	Above Range
50%	26.1 ± 5.0	Above Range	33.3 ± 7.2	Above Range
70%	405 ± 93	Above Range	668 ± 78	Above Range

weight of 10.5 ± 0.8 g/m^2, which was applied on top of a 6.4 ± 1.5 g/m^2 starch base layer. The durability of the paper coating of the high residual stress "neat" formulation was compared to the low residual stress "plasticized" formulation (20%TEC + 10%PVOH). The durability of paper-coated samples was examined by considering the bending of the coating about the neutral axis of the paper, *i.e.*, folding the paper 180° towards the coating side versus folding the paper away from the coated side. In the latter case, the coating was stretched around the thickness of the paper resulting in a different state of stress than folding the paper towards the coating side. In the uncreased state, both the plasticized and neat formulations are comparable barriers to oxygen (Table 4), with performance suitable for several types of food packaging (Wang et al. 2018) at coating weights of 10 g/m^2 at moderate (40–60%) relative humidity.

Damage occurs in the neat (high residual stress) TOCN coating after folding and creasing the paper towards the coated side. This damage is observable as the striations shown in Fig. 8a and led to excessive oxygen permeation that caused multiple samples of this type to produce oxygen transmission values above the range of the permeation equipment. The surface of the creased plasticized coating folded toward the coating side (Fig. 8b) shows limited distortion at the crease. The lack of apparent damage corresponds to oxygen transmission values similar to the uncreased sample. However, when creasing and folding the plasticized coating around the paper away from the coating side, the material was not ductile enough and cracking occurred. This cracking resulted in excessive oxygen transmission that was above the range of testing of the equipment. The results suggest that reducing the residual stress in CNF films provides a certain amount of durability that may allow it to survive a creasing operation when located near the neutral access of bending in a thin lamination.

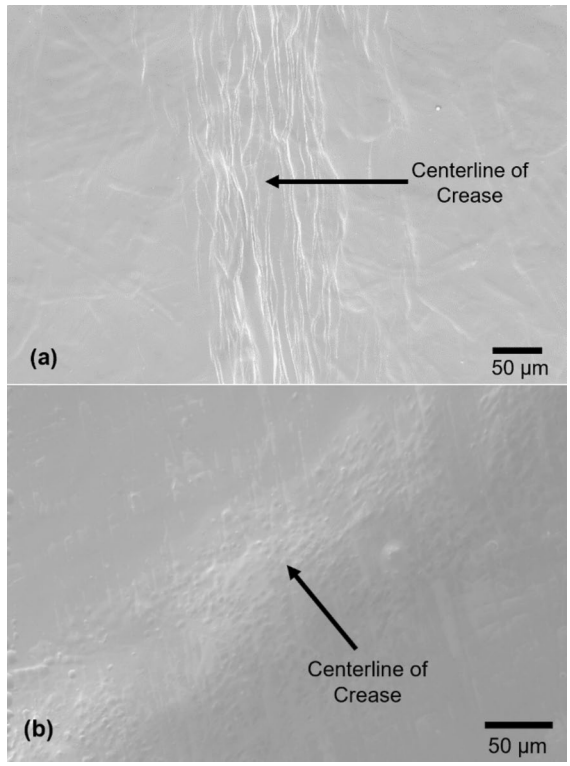

Fig. 8 Scanning electron microscope image of the surface of creased coated paper samples: **a** neat TOCN coating folded toward the coating side of paper, **b** plasticized TOCN coating folded toward the coating side of paper. Note: in both images the arrow is drawn perpendicular to the crease

However, the levels of plasticization examined in this work did not provide enough enhancement in ductility to stretch around paper during bending.

Tensile testing of thin films of TOCNs revealed that neat material had an average strain to failure of 8%, while the TOCNs + 20%TEC + 10%PVOH had an average strain to failure of 18%. The plasticizing effects of TEC combined with PVOH allowed the ductility to increase by a factor of two. However,

Table 4 Average oxygen transmission values in cm^3/m^2·day for paper with 10 g/m^2 coatings of CNF barrier layer in the neat and plasticized (20%TEC with 10% PVOH) state on top of a starch base layer

Relative humidity	TOCNs plasticized uncreased	TOCNs plasticized creased: folded toward coating	TOCNs plasticized creased: folded away from coating	TOCNs neat uncreased	TOCNs neat creased toward coated side
40%	0.7 ± 0.4	0.9 ± 0.5	Above range	1.6 ± 0.4	Above range
60%	12.6 ± 1.2	9.8 ± 0.8	Above range	12.8 ± 1.9	Above range

Note the directionality of the creasing operation with respect to the axis of bending about the paper

material capable of 18% strain to failure does not appear ductile enough to be stretched around the bulk of the paper material during creasing. The reduction in the residual stress should play a role in improving ductility. However, the presence of the plasticizers within the material will also allow for fibrils to slide past each other during deformation, thus increasing the ductility beyond what a reduction in residual stress will achieve on its own. Further investigations on the full understanding of the role residual stress plays on the mechanical properties and durability are needed. Isolating the effect of the residual stress reduction on the ductility of the material would require removing the plasticizer after the structure has formed, which is nontrivial. The residual stress measurement method appears to be a useful tool in the design of more durable CNF layers in flexible packaging.

Conclusions

A new approach was used to examine the durability of CNF films through the lens of quantifying residual stress during drying. It appears that the residual drying stress is not negligible when compared to the yield stress and ultimate tensile stress of these materials. Various plasticizers were examined for their effect on the residual stress. On a mass basis, triethyl citrate (TEC) appears more effective at reducing residual stress than the standard polyols more commonly used to plasticize CNFs (glycerol/sorbitol). This observation was more apparent when the films were subjected to low-humidity environments, as glycerol has a similar effect to TEC at high humidity. The combination of TEC with a small addition of water-soluble polymer (combined total of 30 wt.% of the CNFs mass) led to an approximate 75% reduction in the residual drying stress. In this low residual stress state, thin films (10–15 μm) of TEMPO-oxidized CNFs were able to be creased using the TAPPI T-512 method without any substantial change in oxygen barrier properties when compared to an uncreased neat TOCN film. Creasing neat TOCN films (high residual stress) led to crack formation that caused the oxygen permeation to be above the range of detection. Additionally, 10 g/m^2 coatings of the low residual stress formulation on a 50 g/m^2 basis weight paper were able to be creased when folded toward the coating side and retained their oxygen barrier properties. This suggests that an understanding of the high residual stress formation within CNF films can be useful in understanding the broader concept of durability of CNM films. Further work is needed to fully understand the specific effect of plasticizers and residual stress on mechanical properties that determine coating durability.

Acknowledgements The authors would like to acknowledge Jane O'Dell for performing the DMA tests, Peter Kitin for the SEM imaging, Sara Fishwild and Jim Sheldon for performing the tensile testing, and Richard Reiner for producing the TOCNs.

Author Contributions Daniel Franke formulated the study conception and design. Material preparation, data collection and analysis were performed by Daniel Franke, Ronald Sabo and Cody Schilling. The first draft of the manuscript was written by Daniel Franke and all authors commented on and contributed writing to previous versions of the manuscript. All authors read and approved the final manuscript.

Funding This research was supported by the U.S. Department of Agriculture, Forest Service Forest Products Laboratory. The findings and conclusions in this publication are those of the authors and should not be construed to represent any official USDA or U.S. Government determination or policy.

Data Availability No datasets were generated or analysed during the current study.

Declarations

Conflict of interest The authors declare no competing interests.

Ethical approval Not Applicable.

References

Ahmad Zuber SAN, Rusli A, Ismail H (2019) Effectiveness of triacetin and triethyl citrate as plasticizer in polyvinyl alcohol. Mater Today: Proc 17:560–567. https://doi.org/10.1016/j.matpr.2019.06.335

Arrieta MP, Fortunati E, Dominici F, López J, Kenny JM (2015) Bionanocomposite films based on plasticized PLA–PHB/cellulosenanocrystal blends. Carbohydr Polym 121:265–275. https://doi.org/10.1016/j.carbpol.2014.12.056

Aulin C, Flodberg G, Ström G, Lindström T (2022) Enhanced mechanical and gas barrier performance of plasticized cellulose nanofibril films. Nord Pulp Paper Res J 37(1):138–148. https://doi.org/10.1515/npprj-2021-0061

Azeredo HMC, Mattoso LHC, Avena-Bustillos RJ, Filho GC, Munford ML, Wood D, McHugh TH (2010) Nanocellulose reinforced chitosan composite films as affected

by nanofiller loading and plasticizer content. J Food Sci 75:N1–N7. https://doi.org/10.1111/j.1750-3841.2009.01386.x

Benítez AJ, Lossada F, Zhu B, Rudolph T, Walther A (2016) Understanding toughness in bioinspired cellulose nanofibril/polymer nanocomposites. Biomacromol 17:2417–2426. https://doi.org/10.1021/acs.biomac.6b00533

Bootjomchai C, Laopaiboon R, Pencharee S, Laopaiboon J (2014) Elastic moduli of borosilicate glasses doped with heavy metal oxides. J Non Cryst Solids 388:37–45. https://doi.org/10.1016/j.jnoncrysol.2014.01.039

Chowdhury RA, Nuruddin M, Clarkson C, Montes F, Howarter J, Youngblood JP (2019) Cellulose nanocrystal (CNC) coatings with controlled anisotropy as high-performance gas barrier films. ACS Appl Mater Interfaces 11:1376–1383. https://doi.org/10.1021/acsami.8b16897

Cindradewi AW, Bandi R, Park CW, Park JS, Lee EA, Kim JK, Kwon GJ, Han SY, Lee SH (2021) Preparation and characterization of cellulose acetate film reinforced with cellulose nanofibril. Polymers 13:2990. https://doi.org/10.3390/polym13172990

Corcoran EM (1969) Determining stresses in organic coatings using plate beam deflection. J Paint Technol 41:635–640

Csiszar E, Nagy S (2017) A comparative study on cellulose nanocrystals extracted from bleached cotton and flax and used for casting films with glycerol and sorbitol plasticisers. Carbohydr Polym 174:740–749. https://doi.org/10.1016/j.carbpol.2017.06.103

Erdmann R, Kabasci S, Heim HP (2021) Thermal properties of plasticized cellulose acetate and its β-relaxation phenomenon. Polymers 13:1356. https://doi.org/10.3390/polym13091356

Farooq M, Zou T, Riviere G, Sipponen MH, Österberg M (2019) Strong, ductile, and waterproof cellulose nanofibril composite films with colloidal lignin particles. Biomacromol 20(2):693–704. https://doi.org/10.1021/acs.biomac.8b01364

Fein K, Bousfield DW, Gramlich WA (2021) Processing effects on structure, strength, and barrier properties of refiner-produced cellulose nanofibril layers. ACS App Polym Mater 3:3666–3678. https://doi.org/10.1021/acsapm.1c00620

Fernández-Santos J, Valls C, Cusola O, Roncero MB (2021) Improving filmogenic and barrier properties of nanocellulose films by addition of biodegradable plasticizers. ACS Sustain Chem Eng 9:9647–9660. https://doi.org/10.1021/acssuschemeng.0c09109

Fernandez-Santos J, Valls C, Cusola O, Blanca Roncero M (2022) Composites of cellulose nanocrystals in combination with either cellulose nanofibril or carboxymethylcellulose as functional packaging films. Int J Biol Macromol 211:218–229. https://doi.org/10.1016/j.ijbiomac.2022.05.049

Forti ES, El Awad Azrak SM, Ng XY, Cho W, Schueneman GT, Moon RJ, Fox DM, Youngblood JP (2021) Mechanical enhancement of cellulose nanofibril (CNF) films through the addition of water-soluble polymers. Cellulose 28:6449–6465. https://doi.org/10.1007/s10570-021-03937-0

Greca LG, Klockars KW, Rojas OJ, Tardy BL (2023) Drying stresses to tune strength and long range order in nanocellulosic materials. Cellulose 30:8275–8286. https://doi.org/10.1007/s10570-023-05353-y

Hakalahtia M, Salminen A, Seppälä J, Tammelia T, Hänninen T (2015) Effect of interfibrillar PVA bridging on water stability and mechanical properties of TEMPO/NaClO2oxidized cellulosic nanofibril film. Carbohydr Polym 126:78–82. https://doi.org/10.1016/j.carbpol.2015.03.007

Hansen NML, Blomfeldt TOJ, Hedenqvist MS, Plackett DV (2012) Properties of plasticized composite films prepared from nanofibrillated cellulose and birch wood xylan. Cellulose 19:2015–2031. https://doi.org/10.1007/s10570-012-9764-7

Hasan I, Wang J, Tajvidi M (2021) Tuning physical, mechanical and barrier properties of cellulose nanofibril films through film drying techniques coupled with thermal compression. Cellulose 28:11345–11366. https://doi.org/10.1007/s10570-021-04269-9

Herrera MA, Mathew AP, Oksman K (2017) Barrier and mechanical properties of plasticized and cross-linked nanocellulose coatings for paper packaging applications. Cellulose 24:3969–3980. https://doi.org/10.1007/s10570-017-1405-8

Hubbe MA, Ferrer A, Tyagi P, Yin Y, Salas C, Pal L, Rojas OJ (2017) Nanocellulose in thin films, coatings, and plies for packaging applications: a review. BioResources 12(1):2143–2233

Jung BN, Jung HW, Kang DH, Kim GH, Lee M, Shim JK, Hwang SW (2020) The fabrication of flexible and oxygen barrier cellulose nanofiber/polylactic acid nanocomposites using cosolvent system. J Appl Polym Sci 137:e49536. https://doi.org/10.1002/app.49536

Kelly PV, Gardner DJ, Gramlich WA (2021) Optimizing lignocellulosic nanofibril dimensions and morphology by mechanical refining for enhanced adhesion. Carbohydr Polym 273:118566. https://doi.org/10.1016/j.carbpol.2021.118566

Klockars KW, Greca LG, Majoinen J et al (2023) Drying stresses in cellulose nanocrystal coatings: impact of molecular and macromolecular additives. Carbohydr Polym 303:120465. https://doi.org/10.1016/j.carbpol.2022.120465

Kumar V, Lazarus E, Salminen P, Bousfield DW, Toivakka M (2016) Influence of nanolatex addition on cellulose nanofiber film properties. Nord Pulp Paper Res J 31(2):333–340. https://doi.org/10.3183/npprj-2016-31-02-p333-340

Ma Q, Wang K, Mohawk D, Chen Y, Hazra R, Jiang L (2021) Strong, ductile, transparent, water-resistant cellulose nanofibril composite films via UV-induced inter-cross-linked networks. ACS Sustainable Chem Eng 9:10749–10760. https://doi.org/10.1021/acssuschemeng.1c01222

Mariani LM, Johnson WR, Considine JM, Turner KT (2019) Printing and mechanical characterization of cellulose nanofibril materials. Cellulose 26:2639–2651. https://doi.org/10.1007/s10570-019-02247-w

Mathew AP, Dufresne A (2002) Plasticized waxy maize starch: effect of polyols and relative humidity on material properties. Biomacromol 3(5):1101–1108. https://doi.org/10.1021/bm020065p

MatWeb.com, Borosilicate Glass, Available online: https://matweb.com/search/datasheet_print.aspx?matguid=5bb651ca58524e79a503011b2cd8083d Accessed on 1 March 2024

Mokhena TC, Sadiku ER, Mochane MJ, Ray SS, John MJ, Mtibe A (2021) Mechanical properties of cellulose nanofibril papers and their bionanocomposites: a review. Carbohydr Polym 273(1):118507. https://doi.org/10.1016/j.carbpol.2021.118507

Monfort S, Manas P, Condon S, Raso J, Alvarez I (2012) Physicochemical and functional properties of liquid whole egg treated by the application of pulsed electric fields followed by heat in the presence of triethyl citrate. Food Res Int 48(2):484–490. https://doi.org/10.1016/j.foodres.2012.04.015

Moon RJ, Martini A, Nairn J, Simonsen J, Youngblood J (2011) Cellulose nanomaterials review: structure, properties and nanocomposites. Chem Soc Rev 40:3941–3994. https://doi.org/10.1039/C0CS00108B

Nakamura K, Wada M, Kuga S, Okano T (2004) Poisson's ratio of cellulose Iβ and cellulose II. J Polym Sci B Polym Phys 42(7):1206–1211. https://doi.org/10.1002/polb.10771

Nuruddin M, Chowdhury RA, Szeto R, Howarter JA, Erk KA, Szczepanski CR, Youngblood JP (2021) Structure−property relationship of cellulose nanocrystal−polyvinyl alcohol thin films for high barrier coating applications. ACS Appl Mater Interfaces 13:12472–12482. https://doi.org/10.1021/acsami.0c21525

Payne JA, McCormick AV, Francis LF (1998) In situ stress measurement apparatus for liquid applied coatings. Rev Sci Instrum 68(12):4564–4568. https://doi.org/10.1063/1.1148432

Qing Y, Sabo R, Wu Y, Cai Z (2012) High-performance cellulose nanofibril composite films. BioResources 7(3):3064–3075

Rahman M, Brazel CS (2004) The plasticizer market: an assessment of traditional plasticizers and research trends to meet new challenges. Prog Polym Sci 29:1223–1248. https://doi.org/10.1016/j.progpolymsci.2004.10.001

Reiner RS, Rudie AW (2017) Experiences with scaling-up production of TEMPO-grade cellulose nanofibrils. In: Nanocelluloses: their preparation, properties, and applications, ACS symposium series; American chemical society 1251:227−245. https://doi.org/10.1021/bk-2017-1251.ch012

Reshmy R, Philip E, Vaisakh PH, Raj S, Paul SA, Madhavan A, Sindhu R, Binod P, Sirohi R, Pugazhendhi A, Pandey A (2021) Development of an eco-friendly biodegradable plastic from jack fruit peel cellulose with different plasticizers and Boswellia serrata as filler. Sci Total Environ 767:144285. https://doi.org/10.1016/j.scitotenv.2020.144285

Sabo R, Yermakov A, Law C, Elhajjar R (2016) Nanocellulose-enabled electronics, energy harvesting devices, smart materials and sensors: a review. J Renew Mater 4(5):297–312. https://doi.org/10.7569/JRM.2016.634114

Soni B, Hassan EL, Schilling MW, Mahmoud B (2016) Transparent bionanocomposite films based on chitosan and TEMPO-oxidized cellulose nanofibers with enhanced mechanical and barrier properties. Carbohydr Polym 151:779–789. https://doi.org/10.1016/j.carbpol.2016.06.022

Stoney GG (1909) The tension of metallic films deposited by electrolysis. Proc R Soc London Ser A 82:172. https://doi.org/10.1098/rspa.1909.0021

Tayeb AH, Amini E, Ghasemi S, Tajvidi M (2018) Cellulose nanomaterials—binding properties and applications: a review. Molecules 23:2684. https://doi.org/10.3390/molecules23102684

Tayeb AH, Tajvidi M, Bousfield D (2020a) Paper-based oil barrier packaging using lignin-containing cellulose nanofibrils. Molecules 25(6):1344. https://doi.org/10.3390/molecules25061344

Tayeb AH, Tajvidi M, Bousfield DW (2020b) Enhancing the oxygen barrier properties of nanocellulose at high humidity: numerical and experimental assessment. Sustain Chem 1:198–208. https://doi.org/10.3390/suschem1030014

Teixeira SC, Silva RRA, de Oliveira TV, Stringheta P, Pinto MRMR, Soares NDFF (2021) Glycerol and triethyl citrate plasticizer effects on molecular, thermal, mechanical, and barrier properties of cellulose acetate films. Food Biosci 42:101202. https://doi.org/10.1016/j.fbio.2021.101202

Tian J, Cao Z, Qian S, Xia Y, Zhang J, Kong Y, Sheng K, Zhang Y, Wan Y, Takahashi J (2022) Improving tensile strength and impact toughness of plasticized poly(lactic acid) biocomposites by incorporating nanofibrillated cellulose. Nanotechnol Rev 11:2469–2482. https://doi.org/10.1515/ntrev-2022-0142

Wang J, Gardner DJ, Stark NM, Bousfield DW, Tajvidi M, Cai Z (2018) Moisture and oxygen barrier properties of cellulose nanomaterial-based films. ACS Sustain Chem Eng 6:49–70. https://doi.org/10.1021/acssuschemeng.7b03523

Wedin P, Lewis JA, Bergstrom L (2005) Soluble organic additive effects on stress development during drying of calcium carbonate suspensions. J Colloid Interface Sci 290:134–144. https://doi.org/10.1016/j.jcis.2005.04.020

Yadav M, Rhee KY, Jung IH, Park SJ (2013) Eco-friendly synthesis, characterization and properties of a sodium carboxymethyl cellulose/graphene oxide nanocomposite film. Cellulose 20:687–698. https://doi.org/10.1007/s10570-012-9855-5